

A COMPACT UNDERWATER SHOCK WAVE GENERATOR FOR PRECISE MEDICAL APPLICATION OF SHOCK WAVES

S. H. R. Hosseini and K. Takayama

Biomedical Engineering Research Organization, Tohoku University,
2-1-1, Katahira, Aoba, Sendai 980-8577 Japan

hosseini@ceres.ifs.tohoku.ac.jp

Abstract: Paper reports on production and focusing of micro-underwater shock waves for novel medical applications. A half-ellipsoidal cavity with 20.0 mm minor diameter and the ratio of major to minor diameters of 1.41 was designed and constructed as an extracorporeal shock wave (ESW) source. Underwater shock waves were generated by laser ignition of micro-gram order silver azide pellets ranging from 1.0 to 20 μg . The whole sequences of the shock wave generation, propagation, and focusing were visualized by time-resolved high speed shadowgraph method. Pressure histories were measured at different stand-off distances by using a fiber optic probe hydrophone. It is concluded that the present compact ESW generator has appropriate characteristics for application in precise and sensitive medical procedures.

Introduction

During extracorporeal shock wave therapy (ESWT), shock waves are produced outside the body and are acoustically coupled with the skin, and then propagate in tissue to focus on a targeted area for treatment [1]. This process for the stone fragmentation in medicine is well known as extracorporeal shock wave lithotripsy (ESWL), which has been the most successful medical application of shock waves.

Shock waves have been a common practice for treatment of urinary stones for more than two decades [2]. Recently, applications of underwater shock waves have been extended to various clinical therapies [3], e.g., in orthopedic surgery for bone formation [4], for cancer therapy and enhancement of chemotherapeutic effects [5, 6], for revascularization of cerebral thrombosis [7, 8], and for drug delivery [9, 10].

The first medical application of micro-explosion for direct blasting of bladder stones was carried out by Watanabe and Oinuma [11]. Micro-explosive and double exposure holographic interferometric visualization have been used for ESWL studies in our laboratory since 1980 [12, 13].

The non-invasive or less-invasive approach of shock wave therapy makes it very attractive for therapeutic purposes. For applying shock waves to sensitive medical procedures like cranioplasty in a close vicinity of the brain or for control of pain, generation of underwater micro shock waves plays an

important role [14]. Such delicate applications make limits on usage of conventional and commercial underwater shock wave sources. Therefore, in the present research a compact ESW reflector has been designed and studied. The use of micro-gram order explosive as shock wave source made it possible to produce a variety range of underwater shock waves suitable for in-vivo experimental studies.

Materials and Methods

In our previous experiments [15] several configuration of ellipsoidal cavities for shock wave focusing were examined and it was found that reflectors with major to minor diameters from 1.4 to 1.5 could produce favorable higher focused pressures for medical applications. It was shown that for shallow reflectors the paths of the focusing waves are long and might be disturbed whereas for the more closed forms the paths are short with large convergence angle. In Aachen, Germany [16], the influence of different portion of the ellipsoid on the shock focal zone was studied.

In the present study we constructed a compact optimized shock wave generator with a half-ellipsoidal cavity of 20 mm opening diameter and the ratio of major to minor diameters of 1.41. The shock wave reflector was made of brass. Figure 1 shows the reflector. A diverging spherical shock wave is produced in the first focal point F_1 , partly reflects from the cavity and exit from the reflector. The non-reflected part diverges and propagates first, and then the reflected portion converges toward the focus F_2 . An expansion wave is produced by shock wave diffraction over the exit edge of the reflector, catches up with the outer part of the converging shock and reflects from the axis.

To generate spherical shock waves, silver azide pellets (AgN_3 , 99.9 % purity; 3.77 g/cm^3 , Chugoku Kayaku Co., Ltd., Japan) ranging from 1.0 to 20.0 μg (0.1 μg scatter in weight) were detonated at the first focal point F_1 inside the cavity. Silver azide, AgN_3 , is a photosensitive white crystalline solid. It is insoluble in water and organic solvents. On exposure to light, silver azide turns first violet and finally black, as colloidal silver is formed and nitrogen evolves. The micro-gram charges were manipulated from 10 mg silver azide pellets with a sharp bamboo blade. A microscopic photograph of a 1.0 μg AgN_3 crystal is shown in Fig. 2. The shape of the micro-gram charges was irregular.

To ensure the exact positioning of pellets in F_1 , four 0.5 mm holes were drilled on the reflector's wall facing F_1 , as shown in Fig. 1. The holes were covered by PMMA clear plastic windows. A weak CW He-Ne laser light of 0.2 mW power and 635 nm wavelength was used for the positioning. The pellet was pasted with acetone-acetocellulose to the polished end of a 0.4 mm core diameter optical fiber and was ignited by irradiation of a Q-switched Nd:YAG laser beam (1064 nm wavelength, 7 ns pulse duration, 3.2-mm-diameter beam, total energy 25 mJ/pulse). The total energy of a 10 μ g pellet is about 19 mJ whereas less than 0.4 mJ of laser energy is used for the ignition. The shape of the shock wave, immediately after the explosion of the pellet, is never spherical but shows a three-dimensionally deformed shape [17]. With propagation, it rapidly converts to a spherical shape.

A stainless steel chamber of 500 mm X 500 mm X 500 mm dimensions equipped with 300 mm diameter observation windows and filled with degassed water was used for experiments. Pressures were measured with a fiber optic probe hydrophone of 100 μ m core diameter glass optical fiber and 3 ns rise time (FOPH 2000, RP acoustics, Germany) at the shock focusing area F_2 . The pressure sensor's response time is short enough to accurately capture the peak pressure value at the shock front. The measuring surface of the pressure gauge faces the incident shock wave, so that the shock face-on pressure is recorded.

High speed time-resolved shadowgraph method was used for the flow visualization. A flash-lamp was used as an intense light source. The source light was diffused and diverged by transmitting through a diffusing glass plate, collimated by a 300 mm diameter parabolic mirror, and illuminated the test section. By using an image converter camera (Imacon 468, DRS Hadland LTD) eight images were recorded in each experiment. Simultaneously with the time-resolved shadowgraph visualization, focal pressure at F_2 was measured and recorded.

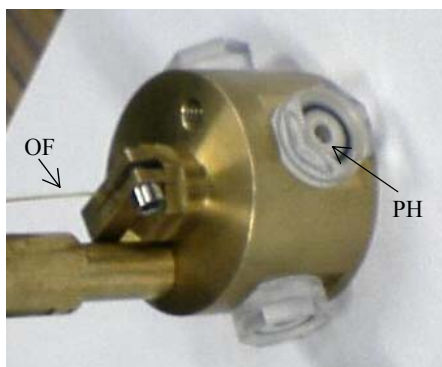


Figure 1: Photograph of 20.0 mm diameter half-ellipsoidal shock reflector. OF, optical fiber; PH, positioning hole

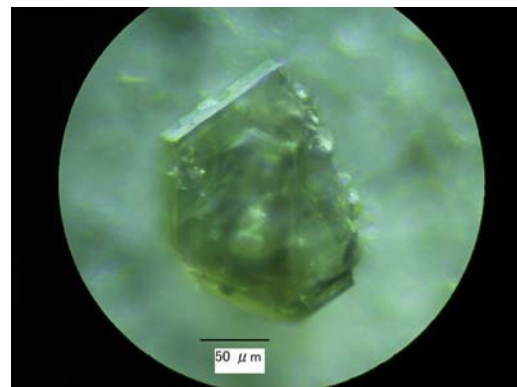


Figure 2: Microscopic photograph of a 1.0 μ g AgN_3 crystal

Results and discussion

Figure 3 shows pressure histories measured by the fiber optic probe hydrophone at the focus F_2 , following the detonation of a 2.5 μ g silver azide at the first focal point F_1 . A photodiode was used to monitor the irradiation of the Nd:YAG laser beam which ignited the pellets. The ignition delay of silver azide was found to be less than 1 μ s [18]. The monitored signal indicates the time instant of explosion and was used as a time base to measure the arrival time of the diverging and focused shock wave at the focal point F_2 . In Fig. 3, 18.9 μ s after the ignition, the converging shock wave arrived at F_2 producing a steep pressure jump of 14.6 MPa peak positive pressure, P^+ . It is followed by a tensile wave of 7.3 MPa peak rarefaction pressure, P^- . The focused

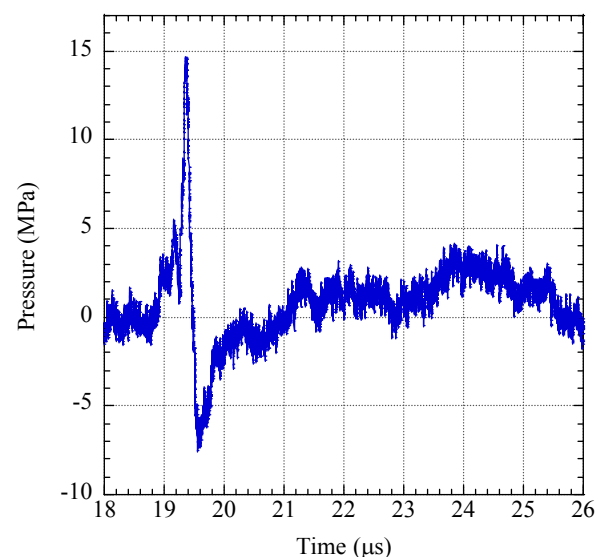


Figure 3: Pressure histories measured at the focus F_2 after explosion of a 2.5 μ g silver azide pellet

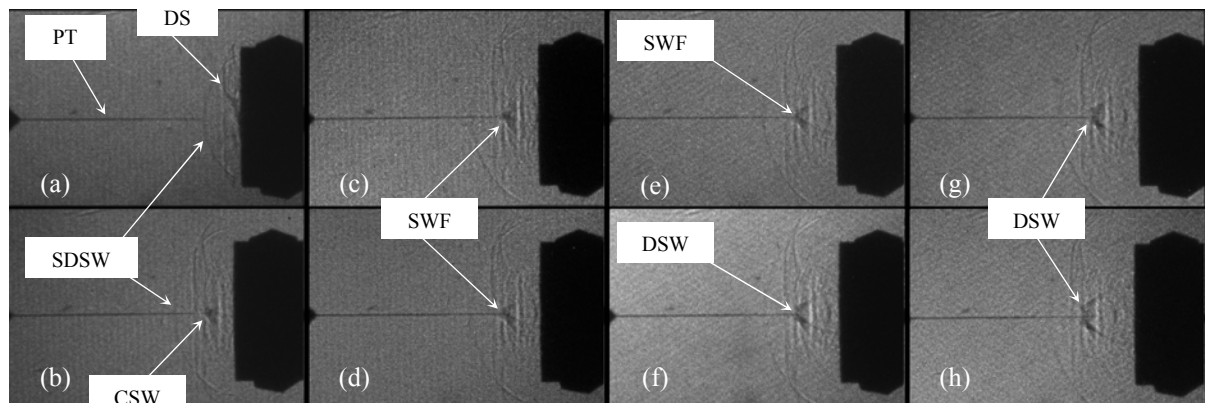


Figure 4: Time-resolved high-speed shadowgraph visualization of shock wave focusing, after the detonation of a 2.5 μg silver azide pellet: (a) 13 μs ; (b) 17 μs ; (c) 18 μs ; (d) 18.5 μs ; (e) 19 μs ; (f) 19.5 μs ; (g) 20 μs ; (h) 21 μs . CSW, converging shock wave; DSW, diverging shock wave after focusing; DS, diffracted shock wave; PT, pressure transducer; SDSW, spherical diverging shock wave; SWF, shock wave focusing

shock wave has a rise time, t_r , (measured from 10% to 90% of P^+) of 70 ns and a pulse width, t_w , (measured from 50% to 50% of P^+) of 120 ns. There is a small compression wave propagating in front of the focusing shock wave. The detonation wave propagating in the micro-gram silver azide in the direction of the laser irradiation takes a time interval of several ten picoseconds, which affects the spherical shape of the diverging shock wave at the very early stage of shock wave propagation and may explain the small compression wave. A small pressure jump at 24 μs apparently corresponds to focusing of a secondary shock wave, produced by the merging of compression waves due to overexpansion following the propagating of rarefaction waves into the explosion products gas. Figure 4 shows eight images of time-resolved high-speed shadowgraph visualization of shock wave focusing, after the detonation of a 2.5 μg silver azide pellet at F_1 , which was recorded simultaneously with pressure measurement of Fig. 3. Each frame had a 250 ns exposure time with a variable inter-frame time. It should be noted that in Fig. 4 axisymmetric flow is visualized. Figure 4(a) shows the spherical shock wave coming out of the cavity, 13 μs after the explosion. A solid line visible from left to the focus F_2 is the optical fiber pressure transducer. In Fig. 4(a) the diverging shock wave before arriving to the optical fiber probe and the diffracted shock wave from the reflector's exit edge are well visualized. Figure 4(b) at 17 μs show the reflected shock wave from the reflector's wall converging toward the focal zone and the rarefaction wave behind the converging shock wave induced by shock diffraction. In Fig. 4(c), at 18 μs , the shock

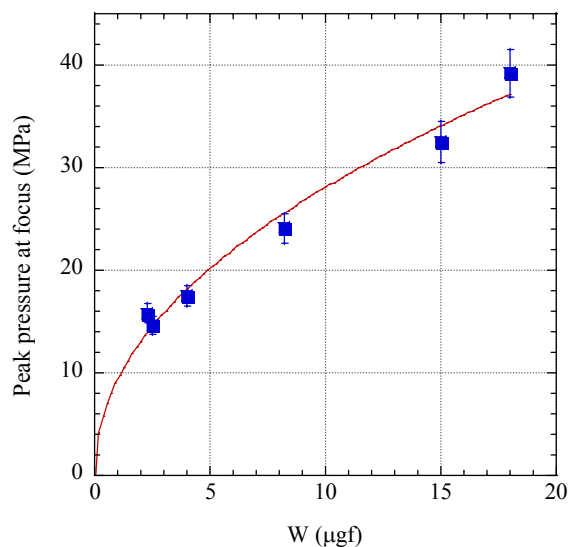


Figure 5: Variation of peak pressure at the focal zone with the charge weight

wave is approaching the focus F_2 . Figures 4(d-e), at 18.5 and 19 μs , show the shock wave in focal zone traversing the optical fiber probe hydrophone pressure transducer. The size of the probe (50- μm -radius) is one order of magnitude less than the shock focal zone of 0.54-mm-radius (lateral direction) observed in Fig. 4(d). Therefore, the probe has a little effect on the flow field. Focal energy E is estimated by integrating the pulse intensity integral (PII) distribution over the 0.54-mm-radius lateral dimension of the focal zone. The focal energy for the positive signal portion E^+ of 2.5 μJ and the complete signal E of 4.4 μJ is obtained, which are at least two orders of magnitude less than the focal energy of the commercial medical shock wave generators. In Fig. 4(f), at 19.5 μs , it is shown that soon after the shock wave focusing, the shock front started diverging. Figures 4(g-h), at 20 and 21 μs , show the propagation of the diverging shock wave after the focus. From image processing of the time-resolved flow visualization of Figs. 4(b-e) a focal extension of 0.54-mm-radius in

lateral direction and 2.3 mm in axial direction is estimated. This evaluation has advantage of minimizing the run to run error, since all of measurements are done in a single shot.

Figure 5 shows the variation of the shock peak pressure at the focal zone with the charge weight. As can be seen from Fig. 5, a wide range of shock positive peak pressure, favorable for medical applications, was obtained.

Conclusions

A half-ellipsoidal cavity with 20.0 mm diameter opening and the ratio of the major to minor diameters of 1.41 was designed and constructed as an extracorporeal shock wave source suitable for medical application of shock waves in sensitive organs. Micro-gram AgN₃ pellets were laser ignited at the first focal point inside the half-ellipsoidal reflector to produce shock wave focusing on the second focal point. A wide range of peak pressures were obtained. It was shown that the present compact underwater shock wave reflector has a focal zone of at least one order of magnitude less than the focal zone of the commercial medical shock wave generators and it has focal energy of two orders of magnitude less than the available therapeutic shock wave sources. These characteristics of the compact shock wave generator make it suitable for novel medical procedures like shock wave administration in the vicinity of the brain for cranioplasty and shock wave application for treatment of neural pain.

References

- [1] HEUSTLER, E. (1975): 'Destruction of kidney stones by means of autofocused guided shock-waves', 2nd European Congress Ultrasonics and Medicine
- [2] DELIUS, M. (2000): 'Lithotripsy', *Ultrasound in Med. Biol.*, **26**, Sup.1, p. S55
- [3] TAKAYAMA, K., and SAITO, T. (2004): 'Shock wave/geophysical and medical applications', *Annu. Rev. Fluid Mech.*, **36**, p. 347
- [4] IKEDA, K., TOMITA, K., TAKAYAMA, K. (1999): 'Application of extracorporeal shock wave on bone: Preliminary report', *J. Trauma*, **47**, p. 946
- [5] KAMBE, M., IORITANI, N., SHIRAI, S., KAMBE, K., KUWAHARA, M., ARITA, D., FUNATO, T., SHIMADAIRA, H., GAMO, M., ORIKASA, S., KANAMARU, R. (1996): 'Enhancement of chemotherapeutic effects with focused shock waves: Extracorporeal shock wave chemotherapy (ESWC)', *In Vivo*, **10**, p. 369
- [6] MOOSAVI-NEJAD, S., HOSSEINI, S.H.R., SATO, M., TAKAYAMA, K. (2005): 'Shock wave induced cytoskeletal and morphological deformations in a human renal carcinoma cell line', *Cancer Science*, to appear
- [7] HOSSEINI, S.H.R., HIRANO, T., ONODERA, O., TAKAYAMA, K. (2000): 'Study of Ho:YAG laser generated underwater shock waves and cavity bubble for revascularization therapy', in Conway T.A. (Ed): 'Advances in Bioengineering', (ASME BED **48**), p. 171
- [8] HIRANO, T., KOMATSU, M., SAEKI, T., UENOHARA, H., TAKAHASHI, A., TAKAYAMA, K., YOSHIMOTO, T. (2001): 'Enhancement of fibrinolytics with a laser-induced liquid jet', *Laser Sur. Med.*, **29**, p. 360
- [9] DELIUS, M., ADAMS, G. (1999): 'Shock wave permeabilization with ribosome inactivating proteins: A new approach to tumor therapy', *Cancer Research*, **59**, p. 5227
- [10] KENDALL, M., MITCHELL, T., WRIGHTON-SMITH, P. (2004): 'Intradermal ballistic delivery of micro-particles into excised human skin for pharmaceutical applications', *J. Biomechanics*, **37**, 1733
- [11] WATANABE, H., OINUMA, S. (1977): 'Studies on application of micro-explosion to medicine and biology. 1. development of special explosive for experiments', *Japanese Journal of Urology*, **68**, p. 243
- [12] TAKAYAMA, K. (1983): 'Application of holographic interferometry to shock wave research', *SPIE*, **398**, p. 174
- [13] KUWAHARA, M., KAMBE, K., KUROSU, S., KAGEYAMA, S., IORITANI, N., ORIKASA, S., TAKAYAMA, K. (1987): 'Extracorporeal micro-explosive lithotripsy – experience of 40 clinical cases', *J. Urology*, **137**, p. 837
- [14] NAKAGAWA, A., KUSAKA, Y., HIRANO, T., SAITO, T., SHIRANE, R., TAKAYAMA, K., YOSHIMOTO, T. (2003): 'Application of shock waves as a treatment modality in the vicinity of the brain and skull', *J. Neurosurgery*, **99**, p. 156
- [15] TAKAYAMA, K. (2003): 'Focusing of shock waves and their applications to medicine', in Srivastava R.C., Leutloff D., Takayama K., Groenig H. (Eds): 'Shock Focusing Effect in Medical Science and Sonoluminescence', (Springer), pp. 121-149
- [16] GROENIG, H. (1989): 'Past, present and future of shock focusing research', *Proc. Intl. Workshop on Shock Wave Focusing*, Takayama K. (Ed), Sendai Japan, pp. 1-37
- [17] HOSSEINI, S.H.R., TAKAYAMA, K. (2005): 'Implosion of a spherical shock wave reflected from a spherical wall', *J. Fluid Mech.*, **520**, p. 223
- [18] MIZUKAKI, T. (2001): 'Quantitative visualization of shock wave phenomena', Ph.D. Thesis, Tohoku University, Japan